DOI: 10.13009/EUCASS2022-7288
9TH EUROPEAN CONFERENCE FOR AERONAUTICS AND SPACE SCIENCES (EUCASS)

Mass Estimation of an Electric Pump Cycle Engine for 30kN-class Upper Stage Launch Vehicle Based on a Battery Technology

Jungyeom Kim[1], Geon Young Kim**[1], Hyoung Jin Lee***[2], Hwanil Huh****[3†]*

[1]Department of Aerospace Engineering, Graduate School of Chungnam National University, Daejeon, 34134, Republic of Korea

[2]Department of Aerospace Engineering, Inha University, Incheon, 21999, Republic of Korea

[3]Department of Aerospace Engineering, Chungnam National University, Daejeon, 34134, Republic of Korea

** kyskjg2002@naver.com*

*** kbky0223@naver.com*

**** hyoungjin.lee@inha.ac.kr*

*****† hwanil@cnu.ac.kr*

Abstract

In this paper 30 kN class LO_X/LCH_4 upper stage engine, mass estimation at the optimal combustion time was analyzed according to a battery. As a result, an electric pump cycle engine showed that 3.76% decrease of mass compared to a gas generator cycle at a condition of 3.5 MPa chamber pressure, 719 s burning time. In summary, considering a 30 kN class LO_X/LCH_4 upper stage launch vehicle engine and recent battery technology, an electric pump cycle has an advantage of mass from burning time of 607 s and longer.

1. Introduction

Due to the recent increase in demand for small satellites, small launch vehicles capable of flexible launches compared to large launch vehicles are also expected to become competitive platforms. Recently, with the research and development of electric vehicles and electric propulsion aircraft, related technologies such as electric motor and battery performance and light mass technology have developed rapidly, and an electric drive motor has become applicable as a driver of the launch vehicle engine pump.

As shown in Table 1, Rocket Lab successfully launched by applying Rutherford engines that use Lithium-Polymer batteries to Electron 1st stage and 2nd stage. Recently, attention has been focused on the electric pump cycle as it has successfully re-entered for reuse.

Table 1: Electron Launch vehicle parameters[1]

	1st Stage	**2nd Stage**
Engine	1 X Rutherford	9 X Rutherford
Thrust (tonf)	16.2 (Sea) / 19.2 (Vac.)	2.2(vac.)
Isp (s)	303	343
Propellant	LOX/Kerosene	LOX/Kerosene

DOI: 10.13009/EUCASS2022-7288

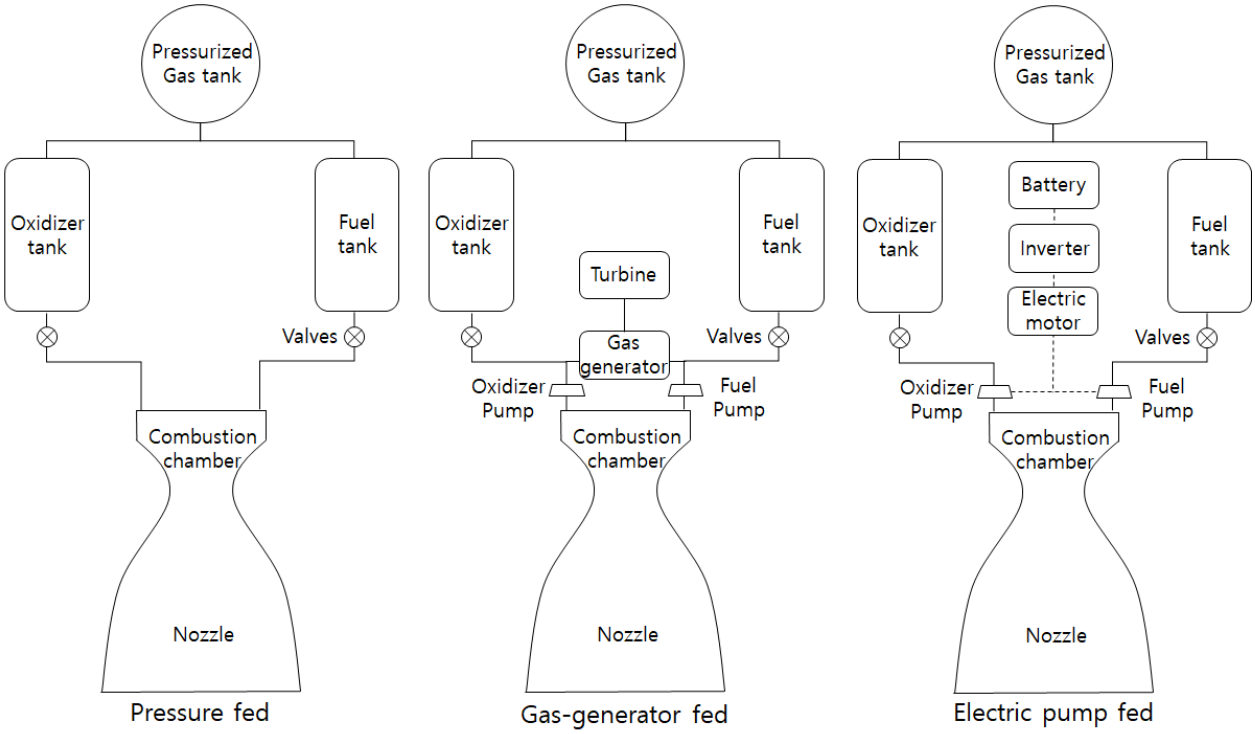

Figure 1: Schematic of three supply systems

A schematic of the three supply systems is shown in Figure 1. An electric pump cycle uses a pump with an electrically driven motor and battery to supply a high-pressure level of propellant to the combustion chamber, which replaces a gas generator and turbine in a gas generator cycle.

According to the study of Kwak et al, the breakdown of engine components of a gas generator cycle and an electric pump cycle are shown in Table 2[2]. This shows that an electric pump cycle has a simple system to reduce the propellant used in additional propellants to drive turbines in a gas generator cycle. Therefore, the tank and propellant mass of an electric pump cycle can be reduced compared to a gas generator cycle, which increases payload capacity. In addition, in an electric pump cycle, a pump is electrically driven by a motor, which has advantageous for rapid ignition and stabilization. Therefore, studies of an electric pump cycle have been conducted in Korea[3-8]. In addition, theoretical mass estimation, component design, and comparative studies with other supply systems are being conducted in many countries. Rachov et al. conducted a comparative study of the liquid propellant rocket engine supply system[9], Vaughan et al conducted a comparative study on the required pressurization performance by considering the pressurization cycle and an electric pump cycle with a 2500 to 4500 N propellant supply system[10]. Juan et al. the mass and development and fabrication cost estimation of the electric pump cycle were studied using historical data[11]. However, mass estimation of an electric pump cycle in previous studies considered a battery type with Lithium-Ion, Lithium-Polymer, and Lithium-Sulfur batteries, but battery technologies are improved significantly fast in recent years. Therefore, estimation of an electric pump cycle engine mass, which applies the latest battery performance, is necessary since it occupies a large part of engine mass in an electric pump cycle. In this study, the latest battery technologies were considered and mathematically estimated the feed system mass of an electric pump cycle. In addition, engine components such as combustion chamber, nozzle, pipe and valve were included, and the mass of battery in an electric pump cycle was estimated.

Also, the mass of the electric pump cycle and a gas generator cycle were compared at an optimal combustion time by applying the battery applicable to the next-generation electric pump cycle and the expected battery performance in the future.

DOI: 10.13009/EUCASS2022-7288

Table 2: Differences between Gas Generator Cycle and Electric Pump Cycle

Gas generator cycle engine		**Electric pump cycle engine**	
Combustion chamber		Combustion chamber	
Turbo pump	LOX pump	Electirc pump	LOX pump
	Fuel Pump		Fuel Pump
	Turbine		Electric Motor
Gas generator			
Igniters	Pyro starter	Igniters	TEAL
	Gas generator igniter		
	TEAL		
Valves	Main oxygen valve	Valves	Main oxygen valve
	Main fuel valve		Main fuel valve
	Gas generator oxygen valve		Others
	Gas generator fuel valve		
	Gas generator oxygen control valve		
	Gas generator fuel control valve		
	others		
Assemblies	Brackets	Assemblies	Brackets
	Fasteners		Fasteners
Controls	Acceleration	Controls	Acceleration
	Pressure		Pressure
	Temperature		Temperature
			Inverter

2. Battery technologies

The power density and energy density should be considered when selecting a battery for an electric pump cycle. And the power density is related to the output power of a motor for driving the pump, and the energy density is related to the combustion time. As there is no battery with high both values at the modern technology level, it is necessary to select the battery according to the purpose of use of launch vehicle. Currently available batteries are Lithium-Ion,

DOI: 10.13009/EUCASS2022-7288

Lithium-Polymer, Lithium-Sulfur, and Lithium-Metal batteries. Among them, Lithium-Ion is widely used in electric vehicles and various fields, and technical research and market occupancy are expected to continue until 2030[12]. In the case of the lithium-polymer battery, it is used as the Rutherford engine battery of an electron launcher and has a high power density so it is verified as a battery applicable to an electric pump cycle launcher, but its energy density is relatively low. Figure 2 shows the comparison of the energy density of the lithium-Sulfur battery with other batteries. The lithium-Sulfur battery is a next-generation secondary battery and is one of the battery candidates to replace the lithium-ion battery used in electric vehicles[13]. At the 2018 NASA Aerospace Battery Workshop, Sion Power unveiled the roadmap for the Lithium-Metal battery in Figure 3, and proposed 8 KW/kg high power density cell and 700 Wh/kg high energy density battery cells[14].

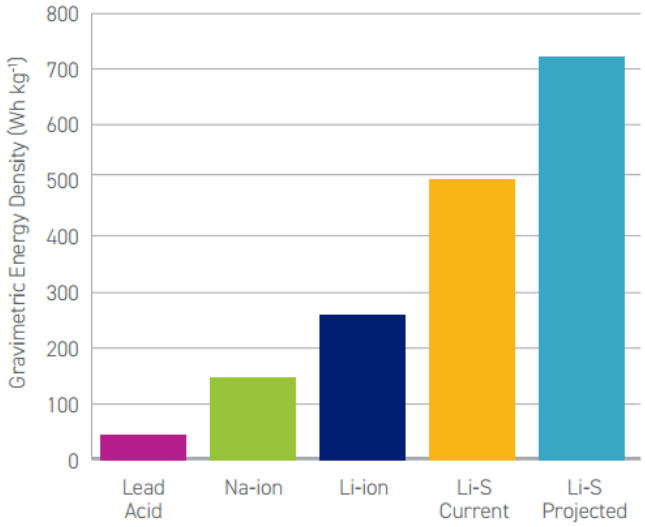

Figure 2: Comparison of the energy density of Li-S batteries to other batteries

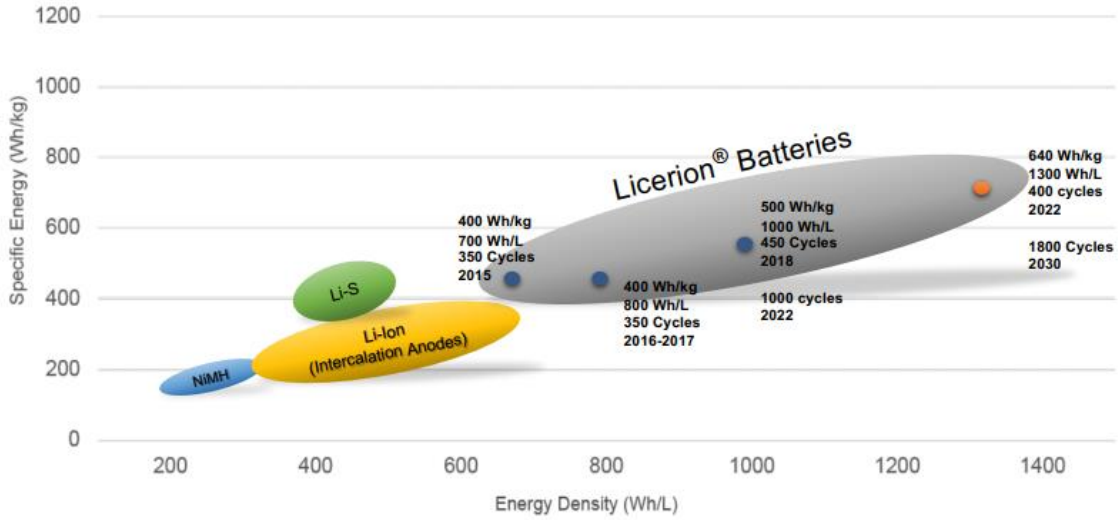

Figure 3: Comparison of energy density of Lithium-Metal batteries and other Batteries

In addition, in the 2020 Technical report, the mass is estimated by comparing the Lithium-Polymer and Lithium-metal batteries with the performance of Table 3 and predicted a mass reduction up to 42 kg compared to the Lithium-Ion batteries in one engine when the Lithium-Metal batteries were applied on a 4 tonf launch vehicle. In addition, the battery mass decreased by up to 50 % compared to the Lithium-Polymer battery of the same performance. Based on this research, Sion Power and NASA discussed the applicability of the next-generation electric pump cycle to batteries[15].

DOI: 10.13009/EUCASS2022-7288

Table 3: Lithium-Metal compared to Lithium-Polymer

Characteristic	Lithium-Metal	Lithium-Polymer
Energy density (Wh/kg)	486	250
Internal resistance (mΩ)	3.5	3.5
Discharge capabilities (C)	15	Up to 70
Operating voltage (V)	4.35 - 3.2	4.2 – 3.0
Capacity (Ah)	20	20

3. Mass estimate

The theoretical mass estimation of an electric pump cycle was calculated through the mass estimation model[9, 16].

$$\boldsymbol{m_{Elec} = m_h + m_{pt} + m_{ot} + m_{ft} + m_{puo} + m_{puf} + m_{em} + m_{inv} + m_{bat} + m_n + m_v + m_{cc}} \quad \textbf{(1)}$$

m_{Elec} represents the total mass of an electric pump cycle, m_h and m_{pt} are the pressurized gas and pressurized gas tank mass, m_{ot} and m_{ft} are the mass of the oxidant and fuel tank, m_{puo} and m_{puf} represent the mass of the propellant pump, m_{em} represents the mass of an electric motor, m_{inv} is the mass of the inverter and m_{bat} is the mass of the battery, m_n is the mass of the nozzle, m_v is the valves mass, m_{cc} is the mass of the combustion chamber. Mass estimation equation of each components are Eq. 2-17.

$$\boldsymbol{\alpha = \alpha_o + \alpha_f} \quad \textbf{(2)}$$

$$\boldsymbol{\alpha_o = \frac{O/F}{\rho_o}\left(\frac{1}{1+O/F}\right)} \quad \textbf{(3)}$$

$$\boldsymbol{\alpha_f = \frac{1}{\rho_f}\left(\frac{1}{1+O/F}\right)} \quad \textbf{(4)}$$

$$\boldsymbol{m_h = k_g k_p k_u \gamma_g \alpha \frac{M_g}{R_u T_0}\left(\frac{m_p P_c}{1-k_p \frac{P_c}{P_o}}\right)} \quad \textbf{(5)}$$

$\boldsymbol{\rho_o}$ and $\boldsymbol{\rho_f}$ are oxidizer and fuel density, $\mathbf{k}_g$ is safety factor for pressuring gas, $\mathbf{k}_p$ is the ratio of tank pressure to combination chamber pressure, $\mathbf{k}_u$ is safety factor to prevent ullage, $\boldsymbol{\gamma_g}$ is pressuring gas specific heat ratio, $\boldsymbol{M_g}$ is molar mass of pressuring gas and $\boldsymbol{R_u}$ is universal gas constant, $\boldsymbol{T_0}$ is initial temperature, $\boldsymbol{P_c}$ is chamber pressure, $\boldsymbol{P_o}$ represents initial pressurized gas pressure.

$$\boldsymbol{m_{ot} = (4\pi)^{\frac{1}{3}} \rho_{ot} (3 k_u \alpha_o m_o)^{\frac{2}{3}} e_{min}} \quad \textbf{(6)}$$

$\boldsymbol{\rho_{ot}}$ is the density of the oxidizer tank material, $\boldsymbol{m_o}$ is the mass of the oxidizer, $\boldsymbol{e_{min}}$ is the minimum thickness of tank wall.

$$\boldsymbol{m_{ft} = (4\pi)^{\frac{1}{3}} \rho_{ft} (3 k_u \alpha_f m_f)^{\frac{2}{3}} e_{min}} \quad \textbf{(7)}$$

$\boldsymbol{\rho_{ft}}$ represents the density of the fuel tank material, $\boldsymbol{m_f}$ is the mass of fuel.

DOI: 10.13009/EUCASS2022-7288

$$\mathbf{m_{puo}} = (\mathbf{1} + \mathbf{k_{pi}} - \mathbf{k_p}) \frac{\mathbf{\alpha_o P_c m_p}}{\mathbf{\delta_{puo} t_b}} \tag{8}$$

$\mathbf{k_{pi}}$ is the ratio of the drop in the injector with respect to chamber pressure, $\mathbf{\delta_{puo}}$ is the oxidizer pump power, $\mathbf{t_b}$ is the burining time.

$$\mathbf{m_{puf}} = (\mathbf{1} + \mathbf{k_{pi}} - \mathbf{k_p}) \frac{\mathbf{\alpha_f P_c m_p}}{\mathbf{\delta_{puf} t_b}} \tag{9}$$

$\mathbf{\delta_{puf}}$ represints fuel pump power density.

$$\mathbf{m_{em}} = (\mathbf{1} + \mathbf{k_{pi}} - \mathbf{k_p}) \frac{\mathbf{P_c m_p}}{\mathbf{t_b}} (\frac{\alpha_o}{\eta_{puo}} + \frac{\alpha_f}{\eta_{puf}}) \frac{1}{\delta_{em}} \tag{10}$$

$\boldsymbol{\eta_{puo}}$ and $\boldsymbol{\eta_{puf}}$ are the efficiency of oxidizer pumps and fuel pumps, $\boldsymbol{\delta_{em}}$ is electric mptor power density.

$$\mathbf{m_{inv}} = (\mathbf{1} + \mathbf{k_{pi}} - \mathbf{k_p}) \frac{\mathbf{P_c m_p}}{\mathbf{t_b}} (\frac{\alpha_o}{\eta_{puo}} + \frac{\alpha_f}{\eta_{puf}}) \frac{1}{\eta_{em}\delta_{inv}} \tag{11}$$

$\boldsymbol{\eta_{em}}$ is the efficiency of the electric motor, $\boldsymbol{\delta_{inv}}$ is the power density of the inverter.

$$\mathbf{m_{bat}} = \mathbf{max}\,(\boldsymbol{m_{bap}}, \boldsymbol{m_{baw}}) \tag{12}$$

For battery mass estimation, after calculating the mass $\mathbf{m_{bap}}$ by the required power density and the mass by the energy density, the higher mass was selected as the final battery mass.

$$\mathbf{m_{bap}} = (\mathbf{1} + \mathbf{k_{pi}} - \mathbf{k_p}) \frac{\mathbf{P_c m_p}}{\mathbf{t_b}} (\frac{\alpha_o}{\eta_{puo}} + \frac{\alpha_f}{\eta_{puf}}) \frac{\mathbf{k_b}}{\eta_{em}\eta_{inv}\delta_{bap}} \tag{13}$$

$$\mathbf{m_{baw}} = (\mathbf{1} + \mathbf{k_{pi}} - \mathbf{k_p})\mathbf{P_c m_p} (\frac{\alpha_o}{\eta_{puo}} + \frac{\alpha_f}{\eta_{puf}}) \frac{\mathbf{k_b}}{\eta_{em}\eta_{inv}\delta_{baw}} \tag{14}$$

$\boldsymbol{\delta_{baw}}$ is the battery energy density, $\boldsymbol{\delta_{bap}}$ is the battery power density, $\boldsymbol{\eta_{inv}}$ is the efficiency of inverter, $\mathbf{k_b}$ is the safety factor to battery.

$$\mathbf{m_n} = \boldsymbol{\pi \rho_n t_w L_n (r_e + r_t)} \tag{15}$$

$\boldsymbol{\rho_n}$ is the density of the nozzle, $\boldsymbol{t_w}$ is the thickness of the wall, $\boldsymbol{L_n}$ is the length of the nozzle, $\boldsymbol{r_e}$ represents radius of the nozzle exit diameter, $\boldsymbol{r_t}$ is radius of the nozzle throat diameter.

$$\mathbf{m_v} = \boldsymbol{m_{v0}} [(\frac{P_c}{P_{c0}})^{0.3} (\frac{\rho_v}{\rho_{v0}})^{1} (\frac{\sigma_{zul}}{\sigma_{zul0}})^{-1} (\frac{\dot{m}_p}{\dot{m}_{p0}})^{0.625} (\frac{\rho_p}{\rho_{p0}})^{-0.625}] \tag{16}$$

$\boldsymbol{\rho_v}$ represents the material density of values and pipe, $\boldsymbol{\sigma_{zul}}$ is allowable stress, $\boldsymbol{\dot{m}_p}$ is the mass flow of propellant, $\boldsymbol{\rho_p}$ is propellant density and $\boldsymbol{m_{v0}}$, $\boldsymbol{P_{c0}}$, $\boldsymbol{\rho_{v0}}$, $\boldsymbol{\sigma_{zul0}}$, $\boldsymbol{\dot{m}_{p0}}$, $\boldsymbol{\rho_{p0}}$ represent values of reference engines.

$$\mathbf{m_{cc}} = \boldsymbol{\pi \rho_{cc} t_w} [\boldsymbol{2 r_{cc} L_{cc}} + \frac{\pi(r_{cc}^2 - r_t^2)}{tan_{\theta cc}}] \tag{17}$$

ρ_{cc} is the density of the combustion chamber, r_{cc} is the radius of the combustion chamber, L_{cc} is the length of the combustion chamber, θcc is the contraction half angle, r_{cc} is the radius of the combustion chamber. The nozzle mass calculation was assumed to be a bell nozzle with a constant wall, In the case of valves, the exact mass cannot be estimated before the detailed design, so it was calculated as a volume proportional equation through reference engine data[10].

Input parameters are summarized in Table 4. A thrust of 30 kN was considered, and liquid oxygen was used as the oxidizer and methane was selected as the fuel. The mixture ratio and engine specific characteristics were calculated through CEA[17].

DOI: 10.13009/EUCASS2022-7288

Table 4: Input parameters

Parameter	value	Parameter	value	Parameter	value
P_c	3.5 MPa	O/F	3.42	δ_{em}	3.8 kW/kg
δ_{inv}	40.6 kW/kg	δ_{pu}	20 kW/kg	σ_{gt}	1100 MPa
σ_{pt}	250 MPa	ρ_o	1132.8 kg/m^3	ρ_f	423.6 kg/m^3
ρ_{ot}	2850 kg/m^3	ρ_{ft}	2850 kg/m^3	η_{em}	0.88
η_{pu}	0.65	η_{inv}	0.85	k_u	1.08

The material for pressurizing gas tank was selected as Ti-6AL-4V and AL Alloy for the propellant tank. It was assumed that the temperature of the pressurizing gas was 100 k and the initial pressure of the pressurizing gas was 27 MPa.

4. Results and conclusion

Batteries used for mass comparison are summarized in Table 5[18-22]. Lithium-Ion, Lithium-Polymer, Lithium-Sulfur and Lithium-Metal are commercial batteries, and the Lithium-Sulfur (2050) is the expected future performance.

Table 5: Battery parameters

Battery	Lithium-Ion [18]	Lithium-Polymer[19]	Lithium-Sulfur[20]	Lithium-Metal[21]	Lithium-Sulfur(2050) [22]
Power density (W/kg)	1160	5956	2400	2450	10000
Energy density (Wh/kg)	259	198	400	490	1000

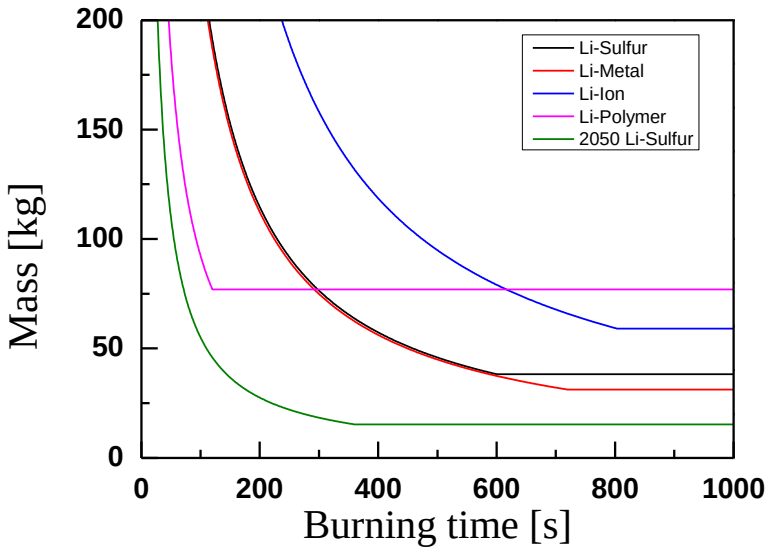

Figure 4: Comparison of battery mass by burning time

DOI: 10.13009/EUCASS2022-7288

Figure 4 shows the graph comparing battery mass according to burning time when a battery in Table 5 is applied to an electric pump cycle. Table 6 summarizes the optimal burning time for each battery to operate at the maximum energy density and the maximum power density and mass at an optimal burning time.
It can be seen that the mass of the battery is determined by the power density at the burning time which is shorter than the optimal burning time as the optimal combustion time, and by the energy density in the opposite case. Except for future Lithium-Sulfur batteries, the highest power density Lithium-Polymer batteries had the lowest battery mass when the burning time was less than 300 seconds, and the highest energy density Lithium-Metal batteries had the lowest mass when it was more than 300 seconds.
In addition, it is expected that when the predictive performance of Lithium-Sulfur is applied in 2050, the battery mass will be significantly reduced because it has a much higher power density and energy density than the existing batteries.

Table 6: Battery optimal burning time and mass

Battery	**Lithium-Ion**	**Lithium-Polymer**	**Lithium-Sulfur**	**Lithium-Metal**	**Lithium-Sulfur(2050)**
Optimal burning time (s)	804	121	600	719	359
Battery mass (kg)	59.02	76.99	38.21	31.24	15.33

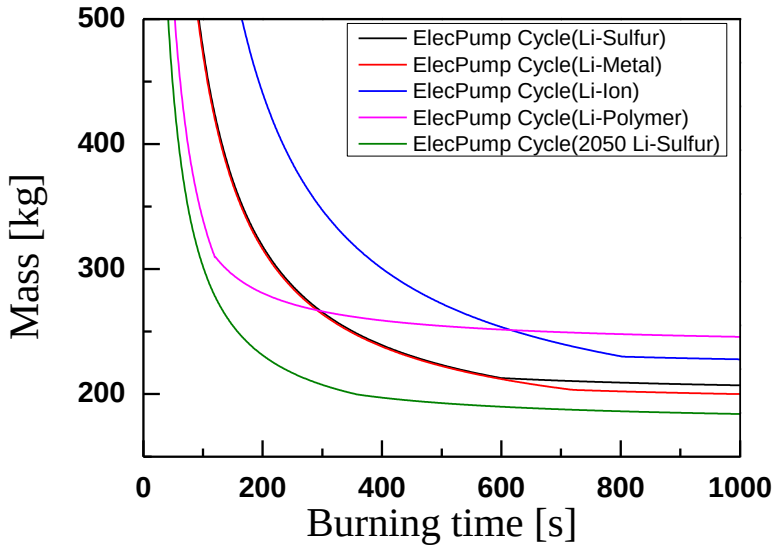

Figure 5: Mass comparison of electric pump cycles by battery selection

Figure 5 is the result of comparing the mass of an electric pump cycle to which each battery is applied. According to the battery mass comparison results, it can be seen that the total mass graph of an electric pump cycle also changes to a similar tendency as the battery mass is constantly fixed at the burning time after the optimal combustion time.
At the optimal burning time of Lithium-Ion, Lithium-Polymer, Lithium-Sulfur, Lithium-Metal, and Lithium-Sulfur (2050), the cycle mass of an electric pump was 229.98, 309.53, 212.87, 203.08, and 199.73 kg and through the Figure 4 and 5, it is possible to minimize the mass of the battery when the burning time is equal to or longer than the optimal combustion time.

DOI: 10.13009/EUCASS2022-7288

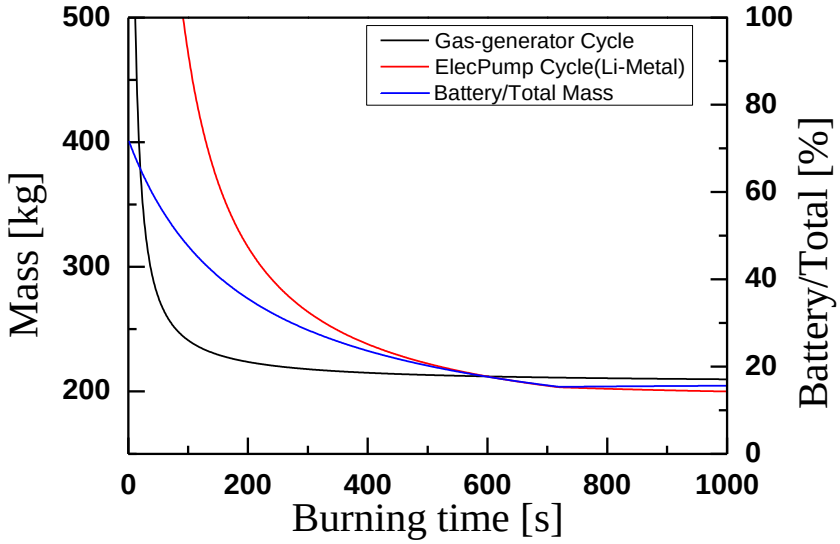

Figure 6: Comparison of mass between gas generator cycle and electric pump cycle with ratio of battery/electric pump cycle mass according to burning time

Figure 6 is a graph comparing the mass of an electric pump cycle and the gas generator cycle to which the lithium-metal battery is applied. At the optimal burning time of the Lithium-Metal battery, an electric pump cycle is 203.47 kg and the gas generator cycle is 211.11 kg, a mass difference of about 7.64 kg occurs, and it can be verified that as the burning time is longer, the mass gain of the electric pump cycle is more significant.

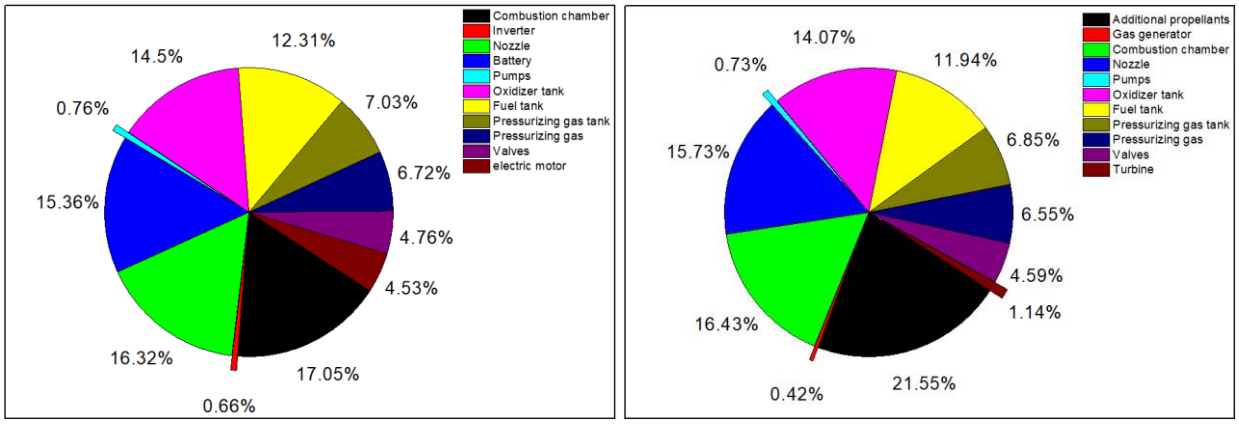

Figure 7: Mass ratio of main components: An electric pump cycle(left) and gas generator cycle(right)

Based on the mass estimation results verified above, it seems necessary to select a proper battery depending on the burning time when applying an electric pump cycle to a launch vehicle.
Figure 7 shows the ratio of the main components of each cycle to the optimal burning time of the Lithium-Metal battery. The battery accounted for 15.36% at the optimal combustion time of 719 seconds, which is a large part of the mass of an electric pump cycle and, according to the battery development, it is expected that the mass gain would increase by applying the electric pump cycle in an upper stage launch vehicle.

5. Acknowledgemen

This work was supported by the National Research Foundation of Korea(NRF) grant funded by the Korea government(MSIT) (NRF-2021M1A3B8078915).

DOI: 10.13009/EUCASS2022-7288

References

[1] Rocket Lab. 2020. Launch:Payload user's guide.
[2] Hyun-Duck, K., and Sejin, K., Chang-Ho, C. 2018. Performance assessment of electrically driven pump- fed LOX/Kerosene cycle rocket engine: Comparison with gas generator cycle. Aerospace Science and Technology 77. 67-82.
[3] Wonkeun, Ki., et al. A Study on Water Flow Testing to Simulate the Propellant Supply System of the Electric Pump Cycle. 2021. Trans. Korean Soc. Mech. Eng. B, Vol. 45, No. 2, pp. 115-124.
[4] Junsub, Choi., et al. Technology and Development Trends of Small Launch Vehicles. 2020. Journal of the Korean Society of Propulsion Engineers. Vol. 24, No. 5, pp. 91-102.
[5] Juyeon, Lee., et al. Performance Analysis and Mass Estimation of a Small-Sized Liquid Rocket Engine with Electric-Pump Cycle. 2021. International Journal of Aeronautical and Space Sciences (2021) 22:94–107.
[6] Wonkeun, Ki., et al. Overseas Research Trends of an Electric-Pump Cycle for Application in Upper-Stage Propulsion Systems. 2020. Journal of the Korean Society of Propulsion Engineers Vol. 24, No. 1, pp. 64-77
[7] Juyeon, Lee., et al. Research Trend Analysis on Modeling and Simulation of Liquid Propellant Supply System. 2019. Journal of the Korean Society of Propulsion Engineers Vol. 23, No. 6, pp. 39-50.
[8] Wonkeun, Ki., et al. Fundamental Experimental Setup of an Electric-pump Cycle for Space Propulsion Systems. 2019. KSPE 2019-2019
[9] Pavlov Rachov, P.A., Tacca, H., Lentini, D. 2013. Electric feed systems for liquid-propellant rockets. J. Propuls. Power 24. 1171-1180.
[10] D. Vaughan, et al. Technology development and design of liquid bi-propellant mars ascent vehicles. 2016 IEEE Aerospace Conference. 1-12
[11] Juan M. Tizón, and Alberto Román. 2017. A Mass Model for Liquid Propellant Rocket. 53rd AIAA/SAE/ASEE Joint Propulsion Conference.
[12] Kim, Y.H., Lim, J.W., Park, G.Y., and Lim, O.T. 2019. Electric Vehicle Market and Battery Related Technology Research Trends. Transactions of the Korean Hydrogen and New Energy Society. Vol. 30, No. 4. 362-368.
[13] THE FARDAY INSTITUTION. 2020. Lithium-sulfur batteries: lightweight technology for multiple sectors. FARADAY INSIGHTS - ISSUE 8: JULY 2020
[14] Y. Mikhaylik., et al. 2018. 650 Wh/kg, 1400 Wh/L Rechargeable Batteries for New Era of Electrified Mobility. 2018 NASA Aerospace Battery Workshop.
[15] Alber Douglawi, Mark Niedzwiecki, and Evan C. Sanders. 2020. Mass Reduction in Space Launch Applications. Technology white paper.
[16] Ronald W. Humble, Gary N. Henry, Wiley J. Larson. 1995. Space Propulsion Analysis and Design. McGraw-Hill Co
[17] McBride, B.J. & Gordon, S. (1992). Computer Program for Calculation and Fitting Thermodynamic Functions, NASA RP-1271
[18] Batemo. LG Chem E66A. https://www.batemo.de
[19] Tattu. TAA22K6S30ASX. https://www.grepow.com
[20] Oxis Energy. Ultra Light Lithium Sulfur Pouch Cell. https://oxisenergy.com
[21] Sion Power. Licerion battery. https://sionpower.com
[22] René Rings, et al. 2019. Sensitivity Analysis of General Aviation Aircraft with Parallel Hybrid-Electric Propulsion Systems. Asia-Pacific International Symposium on Aerospace Technology